Max-Planck-Institut für Meteorologie

REPORT No. 242

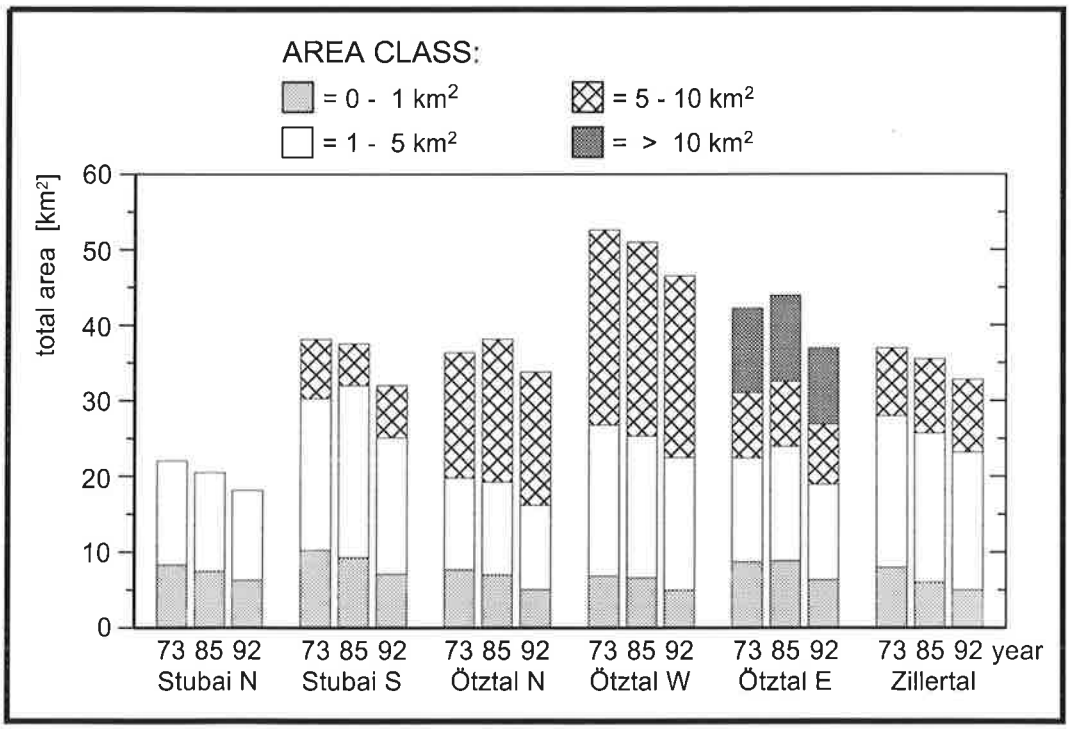

CHANGES OF GLACIER AREA IN THE AUSTRIAN ALPS BETWEEN 1973 AND 1992 DERIVED FROM LANDSAT DATA

by

Frank Paul

HAMBURG, September 1997

AUTHOR:

Frank Paul

Max-Planck-Institut
für Meteorologie

MAX-PLANCK-INSTITUT
FÜR METEOROLOGIE
BUNDESSTRASSE 55
D - 20146 HAMBURG
GERMANY

Tel.: +49-(0)40-4 11 73-0
Telefax: +49-(0)40-4 11 73-298
E-Mail: <name> @ dkrz.de

ISSN 0937-1060

ISSN 0937-1060

Changes of glacier area in the Austrian Alps between 1973 and 1992 derived from Landsat data

Abstract

Data from Landsat satellite sensors are used to obtain an inventory of 165 Austrian glaciers and their temporal change. Applications and modifications of existing remote sensing algorithms for glacier classification are discussed. A trend analysis of the glacier area from a Landsat MSS scene (208/27, Sep. 13, 1973) and two TM scenes (193/27, Sep. 30, 1985 and Sep. 17,1992) reveals:

- Glaciers with areas below 1 km^2, usually excluded from direct observations, shrank significantly by 25 percent between 1973 and 1992.
- There is a strong decrease of glacier area between 1985 and 1992 for glaciers of all sizes.
- Decrease depends on exposition, with highest values found for glaciers exposed to the south and east.
- Accumulation and ablation zones of glaciers are distinguishable by remote sensing, so that the annual net mass balance may be estimated remotely.

1. Introduction

The world-wide retreat of mountain glaciers since 1850 is one of the clearest signals of an on-going global warming. In contrast to the large ice sheets (Antarctica, Greenland), which have an active influence on climate, mountain glaciers react to climatic changes. They integrate over time depending on their size. Thus they smooth out high frequency atmospheric variations and convert a gain of snow of a few meters in depth (after an individual response time) to a change in length of a hundred meters and more (Haeberli, 1995). Therefore glaciers are sensitive climate indicators.

Since 1972, satellites in the Landsat series have been acquiring global data with high spatial resolution. However, there is no global glacier inventory from Landsat data nor has a systematic attempt at documenting the global glacier retreat been published. The present paper reports results of a first attempt to analyse Landsat data for part of the European Alps with algorithms available in literature.

Glaciers are linked to the atmosphere through mass and energy exchange, which determine accumulation (gain of mass) and ablation (loss of mass) throughout the year. At the end of the ablation period, the mass balance is the undelayed reaction to the atmospheric conditions during a year, whereas the change in length (advance or retreat of the glacier tongue) is the delayed reaction to a change in local climate. **Figure 1** outlines the chain of processes.

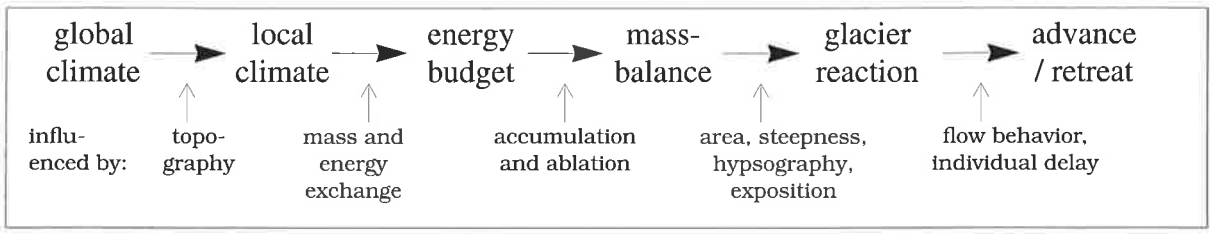

Figure 1: Change in glacier length as a reaction to climate change (after Paterson, 1981).

Different studies have shown high, significant correlations between temperature and precipitation over the year, and the mass balance of a glacier (Kuhn, 1981; Günther and Widlewski, 1986) or the variations of the glacier front position (Gamper and Suter, 1978). Field observations and numerical model studies make it possible to determine the corresponding energy fluxes at the glacier surface, permitting a direct comparison with natural or anthropogenic greenhouse forcing (Oerlemanns, 1994; Haeberli, 1995).

Changes in length and area of even small mountain glaciers (cirques) are detectable with sensors in the Landsat series (Della Ventura et al., 1987). Since 1972 the radiometer Multispectral Scanner (MSS) and since 1984 the Thematic Mapper (TM) have been acquiring calibrated data with high spatial resolution (80 m × 80 m and 30 m × 30 m, respectively) and almost global coverage. Furthermore, it is possible to discriminate snow and ice (on photographic products or with digital data), allowing an estimation of the glaciers' mass balance at the end of the balance year (Krimmel and Meier, 1975; Østrem, 1975). This estimation can be accomplished either with the height of the equilibrium line (ELA), where the mass balance is zero, or with the accumulation area ratio (AAR), which is the ratio of the area covered by snow to the whole glacier area (Paterson, 1981).

Paul (1995) applied the algorithms to 377 glaciers in the European Alps to derive the changes in area between 1973, 1985 and 1992, in an attempt to document general trends in the glaciated area. Therefore, cloud-free Landsat MSS and TM scenes were selected for the end of the ablation period (MSS scene 208/27 from Sep. 13, 1973 and TM scenes 193/27 from Sep. 30, 1985 and from Sep. 17, 1992). The results for 165 selected Austrian glaciers and improvements of the algorithms are presented here.

2. Physical Properties

Glaciers are the result of the metamorphosis of snow over many years. Their spectral properties are very similar to those of snow and ice, except for areas where the glacier is covered by debris. During metamorphosis, the grain size increases continuously, so that the smallest grains can be found at the highest elevations of a glacier, the largest ones at the lowest elevation (at the end of the glacier). Furthermore, the liquid water content at the glacier surface increases from top to bottom due to rising air temperature, at least on temperate mountain glaciers (Orheim and Lucchitta, 1987).

The spectral properties of snow were studied *in situ* (Grenfell et al., 1981) and modelled numerically (Warren, 1982). **Figure 2a** shows the modelled spectral albedo of snow for an illumination angle of 60°, infinite snow depth, and four different grain sizes. The reflection of fresh snow reaches 95% in the visible part of the spectrum and is close to a Lambertian reflector. According to Hall et al. (1989), the reflection in this spectral range is virtually independent of grain size, but depends strongly on contamination by soot and dust. With a content of only 10 ppmv desert dust or 0.1 ppmv soot, the reflection decreases by a few percent. In the near infrared (between 0.7 and 1.5 μm), however, reflection decreases drastically with increasing wavelength and with increasing grain size. On the other hand, the dependence of reflection on contamination decreases.

In the spectral range between 1.5 and 2.2 μm, the reflection of snow is very low, whereas it is high for water and ice clouds (**Figure 2b**). Hence, snow and clouds can be discriminated with the TM channel 5 (see **Table 1** for spectral ranges). There is only minor dependence on contamination, but strong dependence on grain size around 1.8 and 2.2 μm (Dozier, 1984).

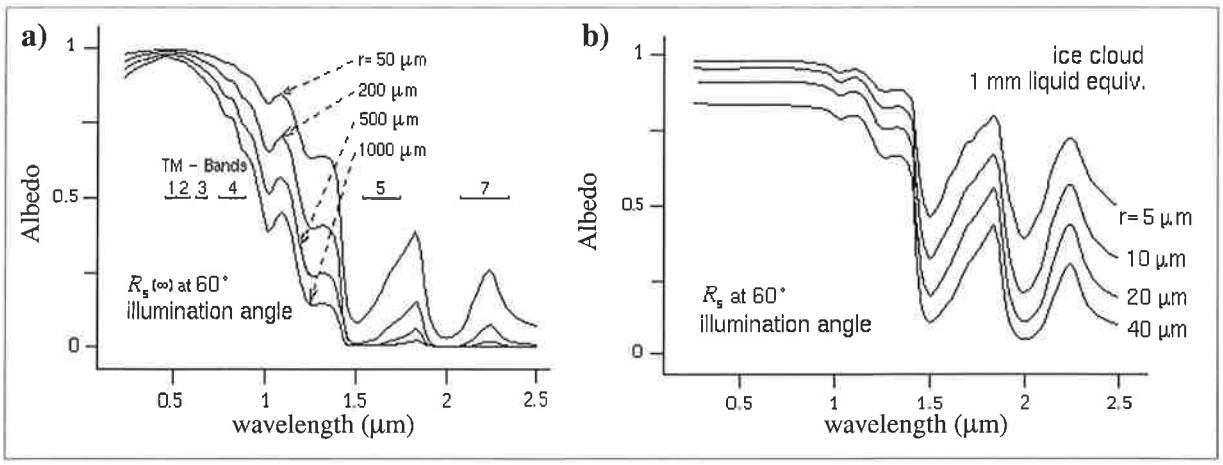

Figure 2: a) Spectral albedo of snow for four grain sizes, infinite snow depth and an illumination angle of 60° (after Dozier, 1989).

b) Spectral albedo for ice clouds with four grain sizes and 1mm liquid water equiv. (after Dozier, 1989).

The algorithms developed for the detection of snow covered areas (SCA) by remote sensing techniques were mainly used to calculate the amount of run-off from snow melt in springtime with numerical models. This quantity is of economic interest for irrigation purposes and power plants. The production of melt water from glaciers is highest in the hot summer months, when water is urgently needed for agriculture, transport, or the reservoirs of hydroelectric power plant (Dozier, 1984).

Channel	1	2	3	4	5	6	7
MSS				0.5 - 0.6	0.6 - 0.7	0.7 - 0.8	0.8 - 1.1
TM	0.45 - 0.52	0.52 - 0.60	0.63 - 0.69	0.76 - 0.90	1.55 - 1.75	10.4 - 12.5	2.08 - 2.35

Table 1: Spectral ranges of the MSS and TM channels in μm (Orheim and Lucchitta, 1987).

The dependence of reflection on snow grain size, and the variation of grain size with glacier facies (ice, slush, snow), mean that different glacier facies can be detected with Landsat (Williams, 1987 and 1991). Comparisons of Landsat-derived snow reflectances with *in situ* measurements showed good coincidence (Hall et al., 1990). In the rugged terrain of mountain areas, a digital elevation model (DEM) may be helpful to distinguish between snow and ice in shadow zones. But often it is possible to separate snow and ice (and other glacier facies) without a DEM (Dozier and Marks, 1987), especially when using the near infrared channels (MSS 7 and TM 4, see **Table 1**).

3. Deriving glacier outlines with Landsat

3.1 Previous Studies

Various earlier applications of Landsat images for the investigation of glaciers used photographic prints from MSS spectral channels. The mass balance was determined at the end of the balance year, when the snow line on glaciers is clearly visible (Krimmel and Meier, 1975; Østrem, 1975; Rott, 1976). Later digital image processing techniques were applied to MSS digital data to delineate different glacier facies in false colour composites (FCCs) (Williams, 1987), or to classify sub-scenes (in snow, glacier and other) with a decision tree classifier (Della Ventura et al., 1987).

Ratios of the TM channels 4 and 5 were also used to separate glaciers from the surrounding terrain (Bayr et al., 1994; Hall et al., 1987 and 1988; Williams et al., 1991). After thresholding the ratio image, a very good glacier mask can be derived, with the exception of debris-covered parts of a glacier or the small, steep glaciers with northwesterly exposition in shadow zones. Furthermore, changes in length

and area were derived from the overlays of the glacier fronts in different years (Bayr et al., 1994; Hall et al., 1992). The comparison with *in situ* measurements showed very good coincidence.

For both the MSS and TM data the algorithms described above have been adjusted to the present task. The MSS and TM scenes were divided into smaller sub-scenes of the same area with a nearly equal glaciation share within each sub-scene. Furthermore a MSS scene from Sep. 17, 1992 (208/27) was used to compare the results of the TM and MSS algorithm directly for a small sub-region.

Only ESA standard geometric corrections are applied to all scenes. Comparing the TM data of 1985 and 1992, there is an offset of one pixel in the north-south direction every 20 km. The MSS data are of poor geographic quality, so that image warping has to be applied before combining MSS and TM data.

3.2 The Thematic Mapper (TM) Algorithm

A 'test area' in the southern "Ötztaler Alps" near the Italian frontier was selected for the development of digital image processing techniques, including the "Hochjochferner" glacier, which was partitioned into four different accumulation basins with different heights. This region shows many important glacial and periglacial features such as thick medial moraines, moraine with varying thickness, areas with snow and bare ice exposed to and away from the sun, steep areas with crevasses, terrain with vegetation, bare rock, and a small lake. **Figure 3** shows the "Hochjochferner" as seen from a nearby mountain on August 17, 1991 for comparison with **Figures 4a - f**, which show different image processing steps.

Figure 3: The "Hochjochferner" in the southern "Ötztaler Alps" as seen from a nearby mountain (17.8.1991). The snow covered areas are white and the glacier ice is grey. The different heights of the four accumulation basins are also recognizable. The areas with snow are similar to those in Figure 4f.

Ratio images from TM channels 4 and 5 were used to derive a glacier mask. Before the ratioing, the digital numbers of both channels were converted from 8 bit integer to 8 bit floating point and the digital numbers (DN) from TM 4 were multiplied by 15. The resulting ratio image was converted back to 8 bit integer and transformed to a binary glacier mask by thresholding.

In **Figure 4a** and **b** TM channels 4 and 5 are shown for the 'test area' after histogram equalization. While glacier ice in TM 4 is light grey and snow is white, in TM 5 the glacier ice appears nearly black and snow in dark grey. The surrounding terrain is dark grey and the vegetation middle grey in TM 4, whereas it is light grey and vegetation white in TM 5. Shaded areas are black in both channels.

Figure 4c is the result of the division of TM 4 by TM 5, yielding high (and similar) grey levels over ice and snow and very low grey levels for the surrounding terrain. In general it is easy to convert the ratio image into a glacier mask by thresholding. The threshold has been varied until more snow and ice pixels than terrain pixels were wrongly classified. The best threshold mostly lies between 2 - 4 grey levels. In **Figure 4d,** the blue and green pixels represent the grey levels that were darker than the threshold and were thus removed (turned to white together with the other even darker pixels). The red and yellow pixels are brighter and were not removed (turned to black).

While removing the terrain pixels by thresholding, the pixels with thick moraines or some snow (ice) in the terrain also disappear. Therefore, the derived glacier areas are somewhat smaller than in reality. To include the moraine covered parts of a glacier, it is possible to mark these areas manually in an FCC, or, if they are quite large, detect them roughly by IHS (Intensity, Hue, Saturation) decorrelation contrast stretching (Gillespie et al., 1986). Further details are discussed in Paul (1995).

After applying a 3×3 median filter to the black and white (binary) glacier mask, some isolated pixels are removed (red in **Figure 4e**) and isolated pixel gaps are filled (blue). If the glaciers are not too small, this produces a better glacier mask, especially in the MSS pictures (see below). The number of pixels added and subtracted to a single glacier by the median filter is similar. The delineation of the glacier mask was derived with a special edge extraction filter, a part of image processing software applied (KHOROS, 1991). In **Figure 4f,** the boundary of the glacier mask is shown in cyan on a TM 3, 2 and 1 (as RGB, respectively) composite image, together with the snow covered area in yellow.

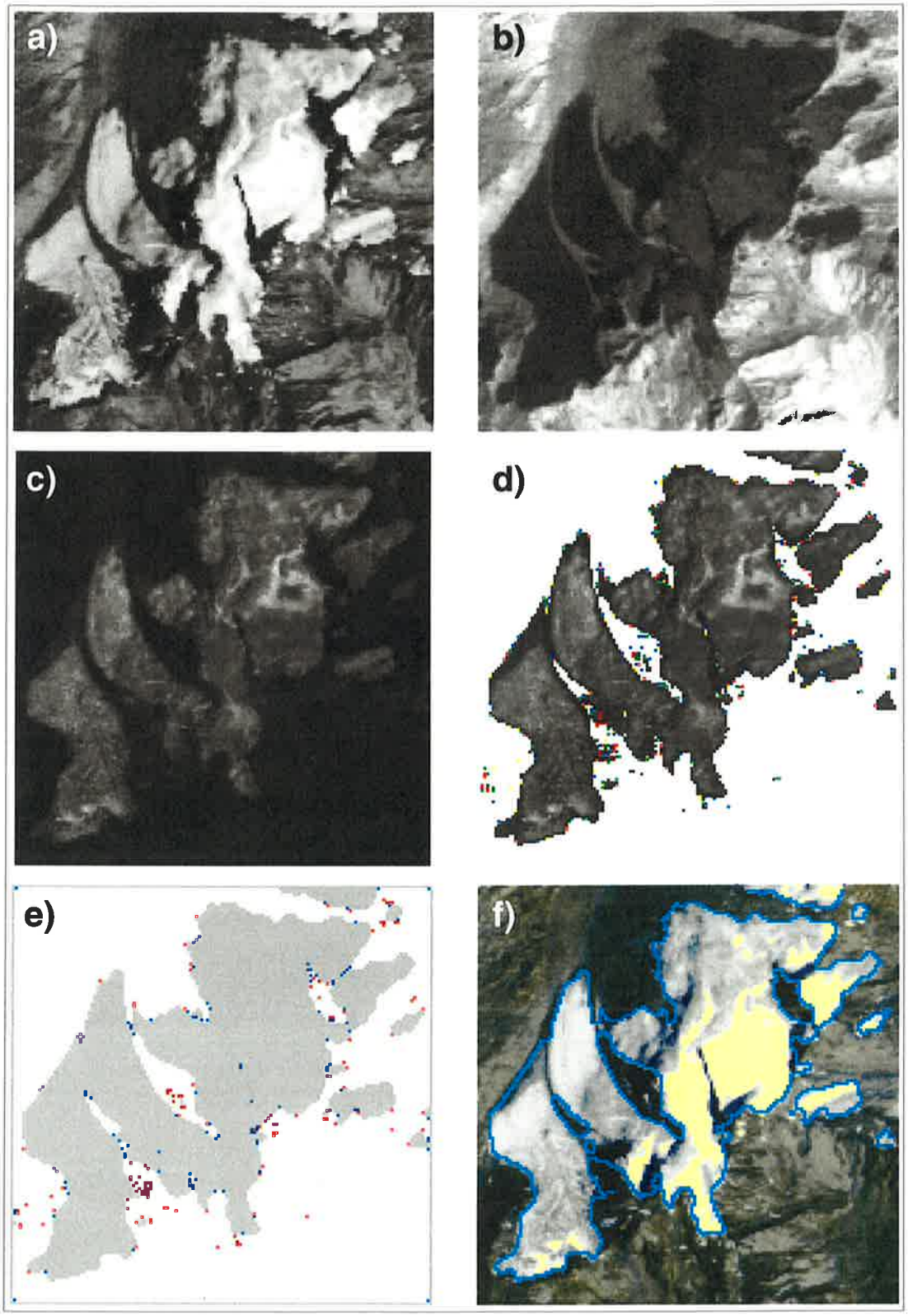

Figure 4: The results of the algorithm for the "Hochjochferner": **a)** and **b)** the region in TM 4 and TM 5 after histogram equalization, **c)** TM 4 / TM 5 ratio image, **d)** the ratio image after thresholding (see text for colours), **e)** the effect of the median filter on the glacier mask (blue pixels were added, red pixels deleted), **f)** glacier boundary (cyan) and snow covered area (yellow) on a composite with TM 3, 2 and 1.

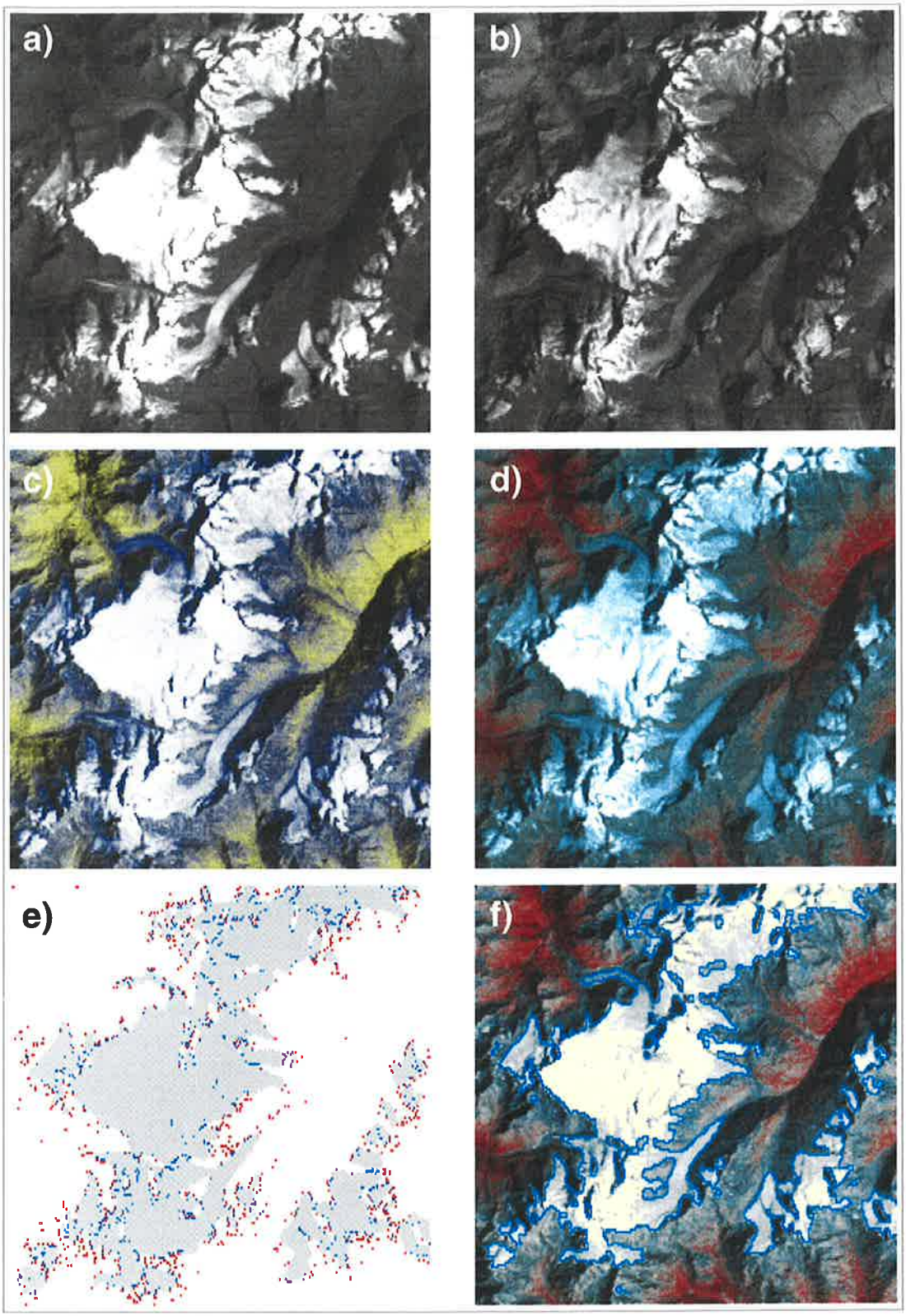

Figure 5: Sub-scene of the southwestern "Ötztaler Alpen" with the "Hochjochferner" in the lower right corner. **a)** and **b)** Subscene in MSS 4 and MSS 7 (raw data). **c)** Composite with MSS 7, 7 and 4 after histogram equalization. **d)** As c), but with MSS 6, 5 and 4 and contrast stretching. **e)** The effect of the median filter on the glacier mask derived from c) (blue pixels were added, red pixels deleted). **f)** Delineation of the glacier margin (cyan) and snow covered area (yellow) on a MSS 6, 5 and 4 composite.

3.3 The Multispectral Scanner (MSS) Algorithm

The *pseudo colouring* of FCCs was used to separate glaciers from the surrounding terrain in MSS scenes, i.e. supervised classification of an unsupervised classification procedure, achieving a reduction of 256^3 classes to 128 colours in the FCC. The three dimensional spectral information about one pixel was converted to a one dimensional class. Because of the small differences in reflection between glacier ice and terrain in MSS 7 and MSS 4, these areas have different colours in the FCC.

Figure 5a and **5b** shows a sub-scene of 15×15 km^2, of the raw data of MSS 4 and MSS 7. Note that the "Hochjochferner" from **Figure 4** is on the lower right. The saturation over snow in MSS 4 and the discrimination of different snow facies with MSS 7 is clearly visible, together with differences in reflection from glacier ice (light grey in MSS 4 and dark grey in MSS 7). The FCC with MSS 7, 7 and 4 (after histogram equalization) is shown in **Figure 5c** and with MSS 6, 5 and 4 (after histogram equalization and contrast stretching) in **Figure 5d**. A fairly good glacier mask is obtained after changing the white, the light grey and most of the blue pixels in **Figure 5c** to black and all others to white. The result of applying a median filter to the binary glacier mask is shown in **Figure 5e**. Here the deleted pixels are red and the new ones are blue. Many of the 'noisy' pixels (from snow patches or misclassification) were removed. The glacier outline was derived with the same edge extraction filter as for TM, and is shown in **Figure 5f** in cyan. The SCA were derived from a FCC similar to **Figure 5d**.

3.4 Snow mapping with TM and MSS

Different algorithms were used to map the snow covered areas (SCA) with TM, . They are mainly based on the reflectance R_p in different TM channels with reflectance thresholds, normalized band ratios ((TM 2 - TM 5) / (TM 2 + TM 5)) and more or less advanced decision tree classifiers (Dozier, 1989). In rugged terrain with glaciers, they generally suffer from illumination effects, because snow in shadow zones has nearly the same reflectance as sunlit ice. Although this kind of snow can be seen in an FCC, automatic mapping is difficult.

TM 1 is often saturated over snow, so that no reflectance can be calculated. Furthermore, taking only the area with saturated pixels will overestimate the real SCAs. In this work, scene-dependent FCCs were used to derive the SCA. These were composed from histogram-equalized and contrast-enhanced composites of TM channels 4, 3 and 2 (MSS 6, 5 and 4) with 128 colours. The SCA were derived from *pseudo colouring* of the FCC by setting the brightest 1 to 6 colours (scene-dependent) white and all others black. Sometimes a second colour (grey) was used to take account of the much darker snow exposed

away from the sun. Snow in shadow zones was not included, but could be marked separately with *pseudo colouring* of a TM 3, 2 and 1 (or MSS 6, 5 and 4) composite, where snow appears light blue. Although this procedure is physically not straightforward, it is quite easy to handle and shows good agreement in comparison with other studies (Rott, 1976; Rott and Markl, 1989).

It should be noticed that in some years, the separation of snow and ice is not easy (even by human eye in an FCC), and would only be carried out correctly with *in situ* measurements or photographic pictures. But when the scenes represent the end of the balance year, end of September, the determination of the mass balance of a large number of glaciers becomes possible (Paul, 1995).

A comparison of the glacier areas and SCA derived with TM and MSS (both scenes acquired on Sep. 17, 1992) is also carried out. The glacier area is somewhat smaller with MSS than with TM, especially for northwesterly exposed glaciers. The SCA varies in the same way so that the AARs are the same.

4. Results and Discussion

4.1 Image handling

A selection of 165 glaciers in Austria was used for a statistical analysis of the results. The data were derived from an MSS scene (208/27) acquired on Sep. 13, 1973 and two TM scenes (193/27), acquired on Sep. 30, 1985 and Sep. 17, 1992. The scenes were subdivided into "Ötztaler Alps" (three regions), "Stubaier Alps" (two regions) and "Zillertaler Alps" including the main glacierized regions. The glacier masks where derived with the algorithms mentioned above and the single glaciers were extracted with freely available X-Tools (X-Paint). The pixels with snow and ice were counted for each glacier and each year respectively. Hence glacier areas (in km^2) were calculated by multiplication with the pixel size of the MSS (57m $\times$ 79m) and TM (30m $\times$ 30m) sensor respectively.

The two problems with thick moraine cover or northwesterly exposed glaciers discussed in previous studies (Bayr et al., 1994; Williams et al., 1991) can be confirmed. The first problem was eliminated by special image processing techniques (median filter) or by hand, and the second by excluding 29 glaciers with northwesterly exposition from statistical analysis (see below).

The classification with TM is fast (50 glaciers per hour) and very accurate (area error $< 1\%$). The MSS algorithm is not so fast (50 glaciers in 5 hours) and not so exact (area error can reach 5%), and the result is influenced by necessary manual operations. The estimation of the SCA (and the AAR) is very fast, but only a first guess, because it depends on exposition.

In addition to the glacier areas for the three years 1973, 1985 and 1992, AARs and changes of area between 1973 - 1985, 1985 - 1992 and 1973 - 1992 were derived for each glacier. Furthermore, the glaciers were separated into four groups of exposition (North, East, South, West) and four area classes (< 1 km^2, 1 - 5 km^2, 5 - 10 km^2, > 10 km^2). Hence numerous combinations of the data are possible.

Figure 6 and **7** represent absolute and relative area changes, sorted into regions, years and area classes respectively. The area classes and groups of exposition were combined with area changes to obtain the results presented in **Figure 8** (see discussion below). **Figure 9** shows the glacier size in 1985 versus change in area between 1985 and 1992 for the five regions. **Table 2** is a summary of the different data for all regions.

To illustrate the loss of glacier area between 1985 and 1992 more clearly, the two binary glacier masks were overlaid and the areas of changes were coloured. They were displayed together with the glacier outline and the SCA in a TM 3, 2 and 1 composite of the sub-scene. A detail of the sub-scene "Ötztal West" is shown in **Figure 10**. The derived glacier area for 1992 is surrounded by a cyan line, the SCA appears in yellow, and the area of changes between 1985 and 1992 in red (loss of area) and green (gain of area), respectively. The calculated properties for the numbered glaciers are shown in **Table 3.**

4.2 Changes in glacier length

Changes in glacier length were derived for three time periods and compared with *in situ* measurements. The changes between 1985 - 1992 are derived for 29 glaciers from a picture similar to **Figure 10**. The pixels in the (red) shrinkage area were counted on lines in the direction of the estimated retreat, and the average was calculated by dividing by the length of these lines. The changes between 1973 - 1985 and 1973 - 1992 were estimated in a different way (for 6 and 15 glaciers, respectively). To match the MSS sub-scene with the corresponding TM scene, interactive image warping with about 16 tiepoints was carried out by an affin transformation. An FCC was created and combined with the glacier outline from the TM scene. The average change in length of a glacier was calculated as described above, but the position of the glacier end in 1973 is only estimated subjectively. Nevertheless it is more accurate than applying the affin transformation to the glacier mask of 1973, because the two algorithms include different parts of debris cover at the glacier end. The average change between 1985 - 1992 is only slightly smaller (8m) than the TM-derived value, with a standard deviation of 18m (about one pixel). No average was calculated for the other two time periods, but the difference for a single glacier can reach values between -90 m and +73 m.

4.3 Area change

4.3.1 Total changes

Obviously from **Figure 6**, the total area of the glacier class smaller than 1 km^2 and of the 1 - 5 km^2 class is nearly the same for all selected regions. In the three sub-regions of the "Ötztaler Alps", the area of the class 5 - 10 km^2 is almost the same if the glacier with 11 km^2 is added. In the sub-regions "Stubai South" and "Zillertal" the proportion of the area class 5 - 10 km^2 is smaller. In the sub-region "Stubai North" this area class is not present. Because of the almost evenly distributed area portions in each class (and also numbers of glaciers), it is possible to compare the relative area changes throughout the regions. This comparison is displayed in **Figure 8**.

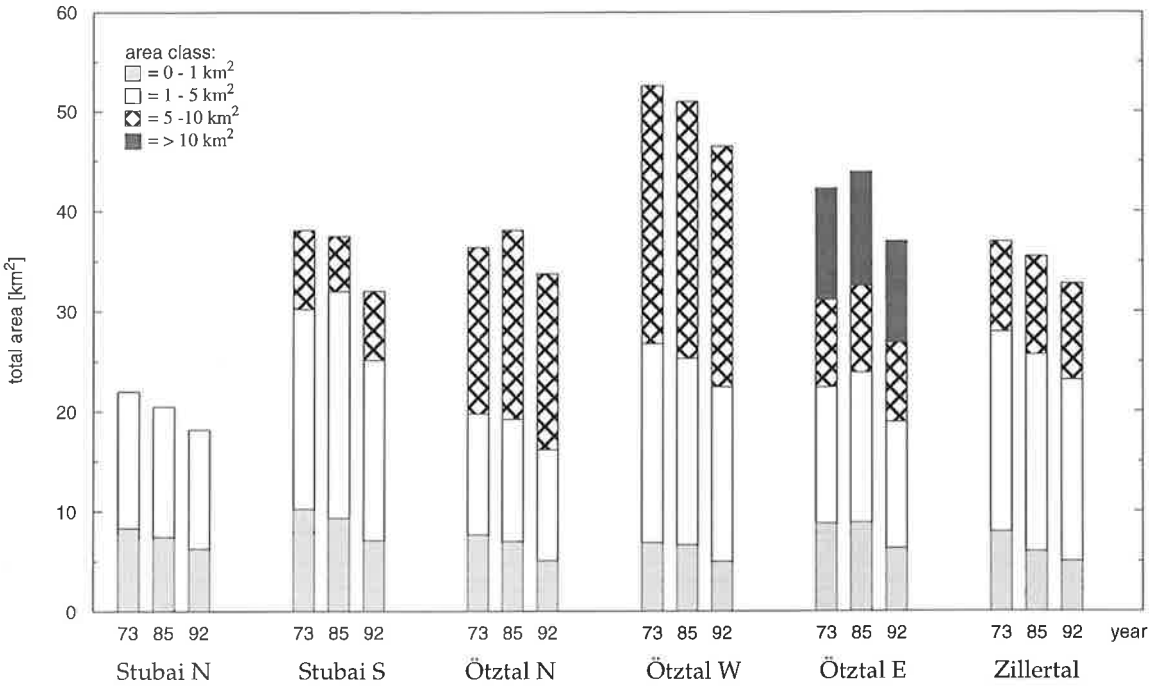

Figure 6: Glacier areas (in km^2) for 1973, 1985 and 1992 for six selected regions and four area classes.

4.3.2 Changes with exposition

Figure 7shows relative area changes versus exposition. Only the glaciers with exposition to the north and west show an increase in area between 1973 and 1985. Between 1985 and 1992 their loss of area is relatively small. Glaciers with easterly exposition have a small loss of area between 1973 and 1985 and a larger one between 1985 and 1992. Glaciers exposed to the south showed nearly the same relative loss of area between the two periods, and a rather great loss (-36%) for the whole period. The average values presented in **Table 2** are indicated in **Figure 7** by an asterix.

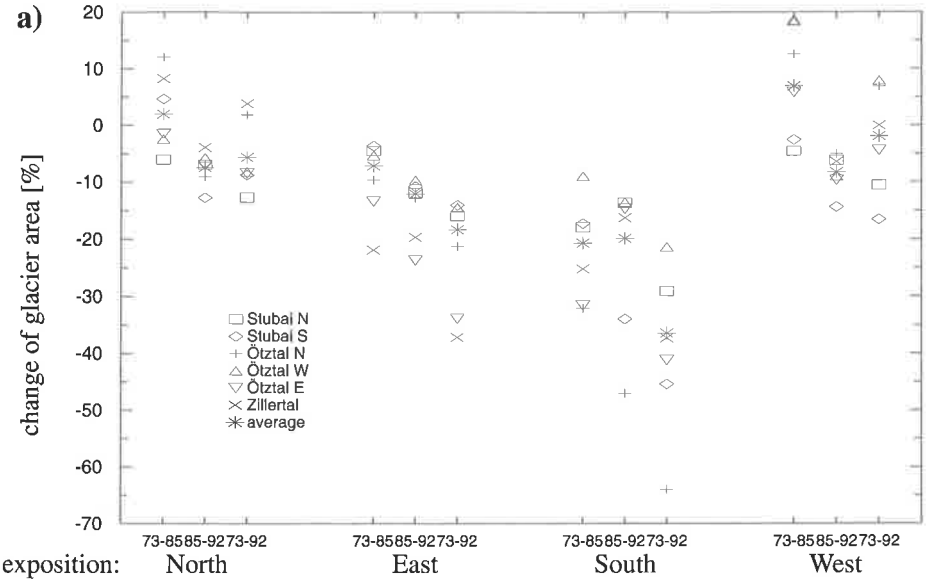

Figure 7: The change of glacier area with exposition for six regions and three different time intervals: A: 1973-1985, B: 1985-1992 and C: 1973-1992.

4.3.3 Relative changes

In **Figure 8** relative changes are presented. All regions have a loss of area in the class < 1km^2 of about -10% between 1973 and 1985, and of about -20% between 1985 and 1992 (with respect to the area of 1985). In the class 1 - 5 km^2, small positive and negative (-7 to +5%) area changes are found between 1973 and 1985 and area losses (-6 to -12%) have occurred between 1985 and 1992. The changes in the classes 5 - 10 km^2 and > 10 km^2 are roughly of the same size and direction, with the exception of the region "Ötztal North" and "Zillertal", where a larger surplus of area can be noted.

In total (all regions and all classes), there is a small loss of area between 1973 and 1985 (3.43 km^2 or - 1.5%), and a large loss between 1985 and 1992 (21.4 km^2 or -9.6%). In total, 24.83 km^2 or -10.9% of the total area of the selected 165 glaciers disappeared between 1973 and 1992. Small glaciers (< 1 km^2) in particular showed a very significant loss of -25.2% of their area in this period.

In this study 29 glaciers with an area of 9.48 km^2 (1992) are excluded from statistical analysis because of poor discerning with the MSS algorithm (small, steep glaciers with northwesterly exposition). With an area of 10.76 km^2 in 1985 they lost -11.9% of their area until 1992. This value is only slightly smaller than the -9.6% for the 165 selected glaciers and will not change this value at all. They account only for 4.5% of the total area and are all smaller than 1 km^2, but they will lower the MSS derived glacier area (6.94 km^2 in 1973) significantly, so that the area of 1973 is somewhat smaller than 1985, resulting in a positive change of area (+0.2%) between 1973 and 1985.

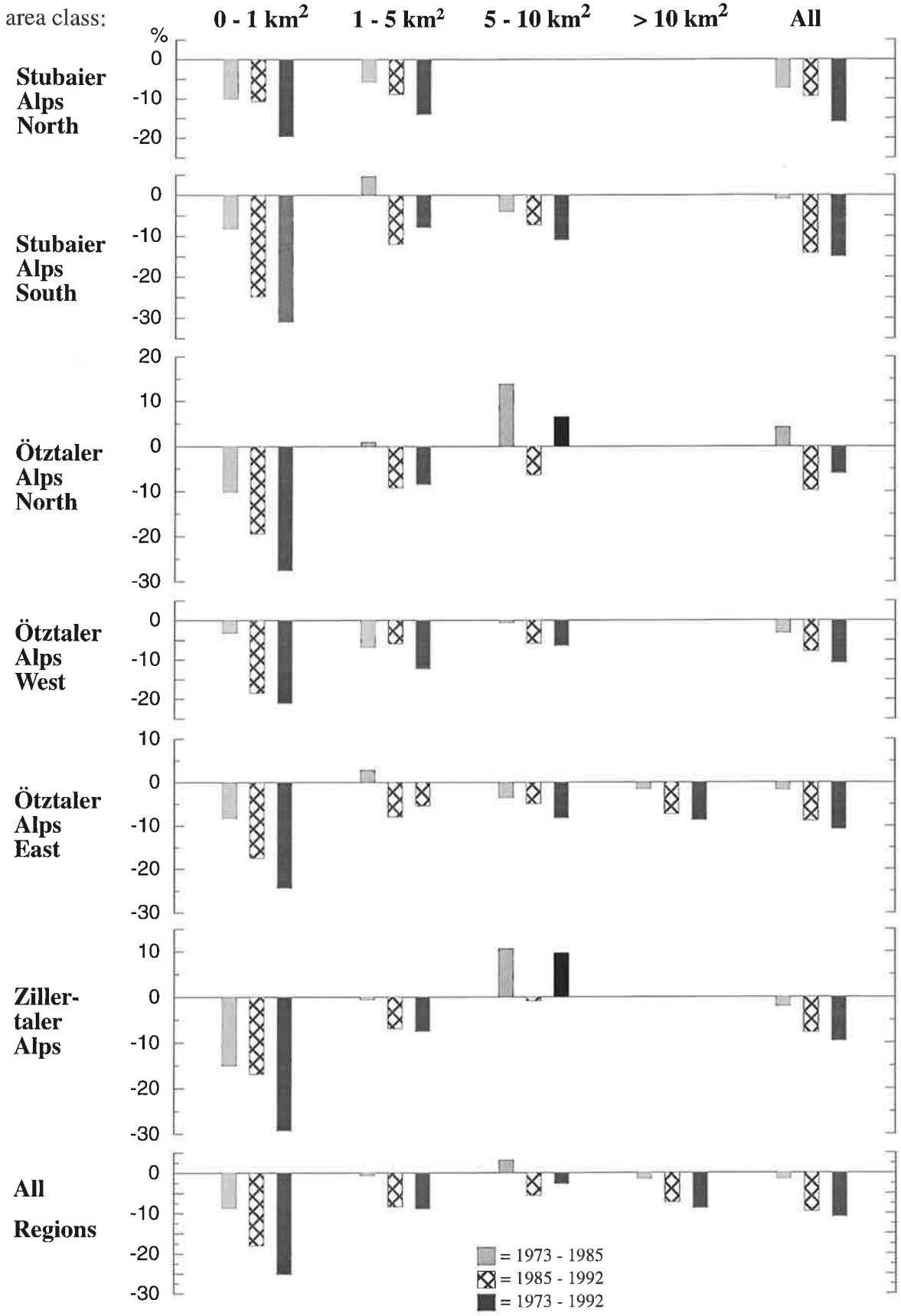

Figure 8: Change of glacier area (as %) for six selected regions, separated into area classes and the time periods 1973 - 1985, 1985 - 1992 and 1973 - 1992.

size interval [km^2]	num-ber	percent of glacierized area			change in area [%]			AAR [%]		
		1973	1985	1992	73 - 85	85 - 92	73 - 92	1973	1985	1992
0 - 1	109	22.0	20.3	18.4	- 8.8	-18.4	-25.7	13	40	25
1 - 5	47	45.1	45.5	46.1	- 0.8	- 8.4	- 9.1	26	40	31
5 - 10	8	28.0	29.3	30.6	+ 3.1	- 5.6	- 2.7	27	43	30
> 10	1	4.9	4.9	5.0	- 1.5	- 7.3	- 8.7	11	40	38
exposition										
North	61	51.6	53.4	54.6	+ 1.9	- 7.5	- 5.8	20	37	27
East	51	24.5	23.0	22.2	- 7.3	-12.0	-18.4	31	57	39
South	25	8.8	7.1	6.3	-20.7	-19.9	-36.4	27	49	44
West	28	15.1	16.5	16.9	+ 7.5	- 8.3	- 1.4	19	28	20
All Glaciers	**165**	**227.21**	**223.78**	**202.38**	**- 1.5**	**- 9.6**	**-10.9**	**23**	**41**	**30**

Table 2: Number, area, area change and AAR for glaciers in Tyrol, Austria. The absolute area is listed in the last row of the columns 'percent of glacierized area'.

Table 2 also indicates the relation between AAR and area class, and between AAR and exposition. No dependence of the AAR on the area class is found and only weak dependence on exposition. As already discussed, the glaciers with exposition to the west and north have the lowest AAR whereas the glaciers with eastern and southern exposition reach twice the value in 1985 and 1992. This clearly demonstrates the dependence of AAR on the direction of sunlight (southeast), and contradicts the behaviour of snow, which lasts much longer when exposed to the north or west (in rugged terrain). So the only conclusion could be that the mass balance of the glaciers is negative in all three years, especially 1973 and 1992. This has also been measured *in situ* (Rott, 1976; Patzelt, 1979 ff).

Figure 9 shows that there is large scatter of relative area changes (0 to -60%) in the smallest glacier class (< 1 km^2), moderate scatter for glaciers between 1 and 3 km^2 (-5 to -20%) and a nearly constant value (-8%) for larger glaciers, confirming other studies over longer time periods (Gross, 1987).

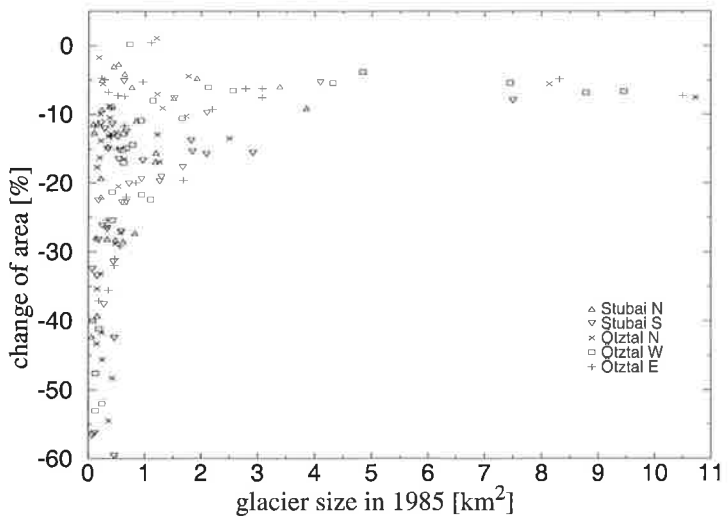

Figure 9: The change of glacier area between 1985 and 1992 versus glacier size of 1985 for five selected regions.

Figure 10 shows a small portion of the southern "Ötztaler Alps" with the area changes between 1985 and 1992. Some isolated red areas show glaciers which disappeared completely between 1985 and 1992. In some cases, these areas are only snow patches, having survived in 1985 but not in 1992. So attention must be paid to the weather conditions before the acquisition date of the scene, especially to snow falls. The red area at the highest point of glacier 22 (a part of the "Niederjochferner") received special attention in 1991, when "Ötzi", the stoneage man, was discovered due to the strong melting of the glacier, partly caused by a strong sahara dust storm in March of the same year, lowering albedo.

		Area [km^2]			Change in Area [%]			AAR [%]			
No.	Glacier	73	85	92	73 - 85	85 - 92	73 - 92	73	85	92	Exp.
1	Plattei	0.19	0.19	0.11	+ 4.6	-41.2	-38.5	14	57	18	O
2	Vernagt	9.68	9.45	8.83	- 2.4	- 6.6	- 8.8	38	52	29	O
3	Großer Guslar	1.72	1.67	1.50	- 2.8	-10.6	-13.1	35	55	33	O
4	Mittlerer Guslar	0.97	0.94	0.86	- 3.6	-8.3	-11.7	10	46	37	N
5	Mittlerer Guslar	0.16	0.17	0.11	+ 6.2	-34.0	-29.9	0	4	0	N
6	Kesselwand	4.23	4.32	4.08	+ 2.1	- 5.5	- 3.5	65	72	69	O
7	Hintereiswände	0.81	0.61	0.52	-24.5	-15.2	-36.0	40	63	54	O
8	Vernaglwand	1.23	0.93	0.83	-24.3	-10.9	-32.6	40	65	49	O
9	Hintereis	8.99	8.78	8.19	- 2.2	- 6.8	- 8.8	30	47	31	N
10		0.45	0.67	0.57	+65.4	-14.9	+40.8	1	15	1	W
11	Latsch	0.23	0.14	0.07	-39.7	-52.9	-71.6	0	42	9	S
12	Steinschlag	0.94	0.95	0.74	+ 1.1	-21.7	-20.8	9	37	12	O
13	Schwemser	0.22	0.26	0.13	+19.2	-51.9	-42.6	6	45	6	O
14	Fineil	0.23	0.14	0.12	-40.1	-15.4	-49.3	11	29	32	S
15	Hochjoch	7.15	7.45	7.04	+ 4.1	- 5.4	- 1.5	9	32	14	N
16	Kreuz, S.	0.74	0.77	0.69	+ 4.0	-10.8	- 7.2	2	24	4	W
17	Kreuz, M.	0.53	0.62	0.55	+16.3	-11.4	+ 3.1	2	17	2	W
18	Kreuz, N.	0.36	0.43	0.35	+19.1	-17.9	- 2.3	0	33	4	W
19	Eisferner	1.07	1.15	1.05	+ 7.1	- 8.0	- 1.5	1	41	20	N
20	Rotkar	0.40	0.42	0.32	+ 4.8	-25.4	-21.8	3	43	4	N
21	Say	0.46	0.40	0.36	-11.7	-10.3	-20.8	15	50	38	N
22	Niederjoch, W.	0.46	0.28	0.20	-39.2	-27.6	-56.0	0	16	7	O
23	Niederjoch	2.47	2.26	2.16	- 8.5	- 4.5	-12.6	12	31	14	N
	whole region	**43.69**	**43.00**	**39.38**	**-1.6**	**-8.4**	**-9.9**	**27**	**46**	**29**	

Table 3: Area, change in area and AAR for the numbered glaciers in Figure 10. Glacier No. 10 was excluded from statistical analysis.

4.4 Error discussion

Several error sources influence the present analysis and will be discussed below. To reduce the impact of snow patches, scenes must be acquired at the end of the ablation season. Therefore the scenes must be carefully selected and the consideration of field measurement data may be necessary.

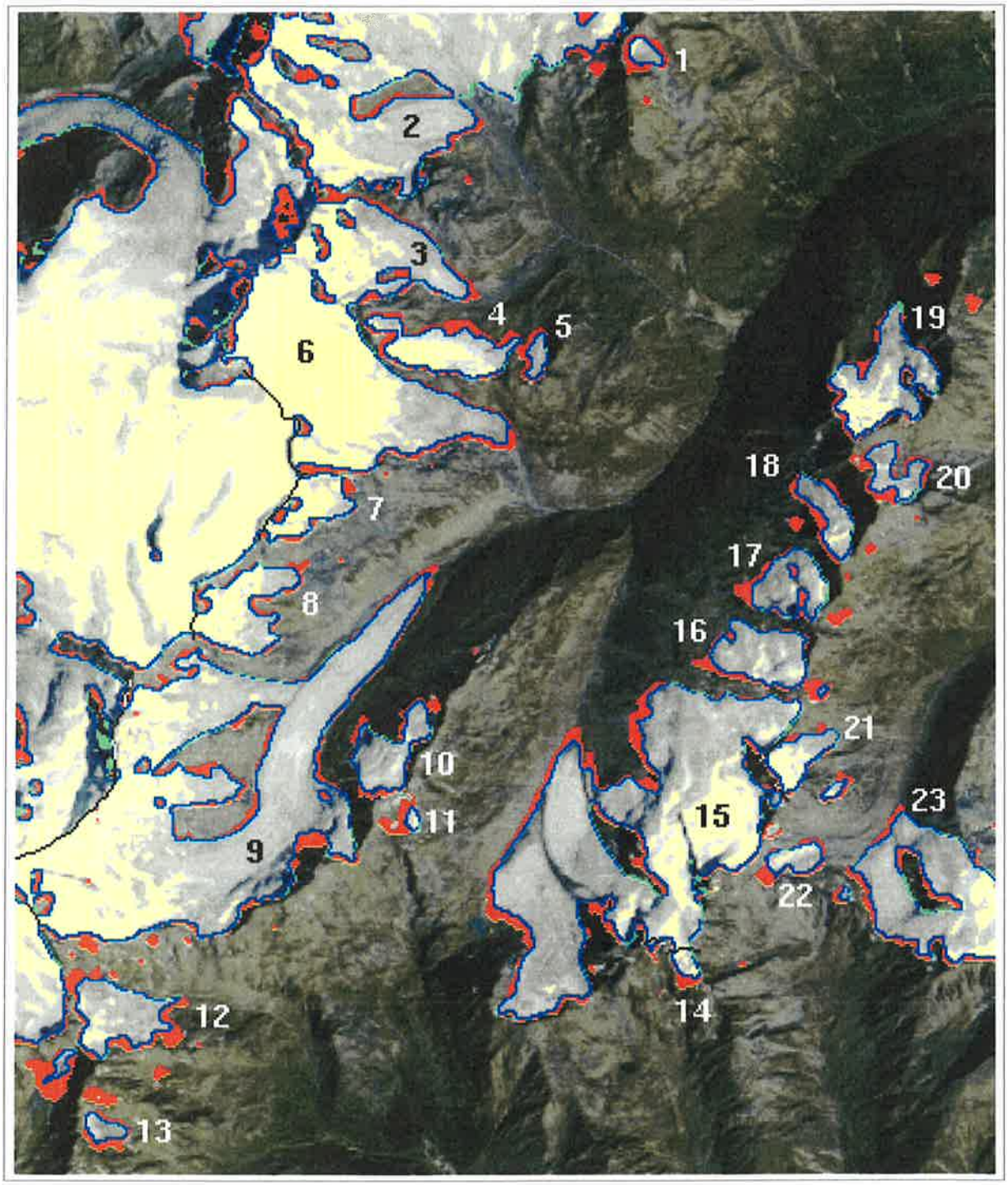

Figure 10: Glacier changes in a small part of the southern "Ötztaler Alps" between 1985 and 1992. The image is the result of combining the digital glacier masks from both years and adding the differences to the TM image 17. Sep. 1992 (band 3, 2 and 1 as RGB). Loss of area is shown in red and gain of area in green. The snow covered area (yellow) and the glacier margin from 1992 (cyan) is also shown. For the glacier numbers see Table 3.

Considerable difficulty is created when large glaciers split into several smaller ones after 1973, especially if the area class changes. In most cases, these glaciers (about 20) were treated as one in the following years, although this is physically not correct. If a glacier moves into another area class due to gain or loss of area, its area class was calculated from the average of all three years.

As discussed by other authors (Bayr et al., 1994; Williams et al., 1991) it is not possible to include a thick moraine on a glacier with the available algorithms. If the debris cover is only one pixel in size and of arbitrary length, the pixel(s) were added to the glacier surface after median filtering. For larger areas it is often possible to detect the moraine in an FCC and mark it by hand.

Sometimes two (or more) glaciers originate from or come together in a single basin without a distinct border. In such cases, the border between them was derived from topographical maps (from scale 1:25000) and laid over the sub-scene before extracting the single glaciers (see glacier 6 in **Figure 10**). GIS orientated digital maps with watersheds may be helpful for further studies. In general, mixed pixels containing snow or ice and terrain are not included and the real glacier size should be somewhat larger.

The derived AARs depend on exposition, and are rough estimates. More sophisticated SCA mapping algorithms or the use of DEMs may be helpful to obtain better results.

With the algorithm for MSS some small glaciers with exposition to the northwest (in shadow zones) where not or only poorly discerned. These 29 glaciers were excluded from statistical analysis.

The separation of the glaciers from the surrounding terrain in MSS scenes with *pseudo colouring* is more complicated than with the TM algorithm. But it is much easier than indicating the glacier area completely by hand.

These error sources may influence details of the results, but they do not corrupt the essential result of a general reduction of glacier area between 1973 and 1992.

5. Conclusion

The ratio between TM channels 4 and 5 was used (after thresholding) to produce a glacier mask. With MSS digital data *pseudo colouring* of FCCs leads to a similar glacier mask. The two algorithms were discussed in previous studies, but applied only to a small number of glaciers. Here they were used for a large number of glaciers in the European Alps to calculate their areas in 1973, 1985 and 1992, and to estimate their mass balance by calculating the AAR. The changes in length could also be estimated with high precision from TM digital data.

The present study supports other findings that Alpine glaciers have been generally retreating within the last 20 years between 1973 and 1992, with increased speed in the last decade. Nevertheless, the advance period of larger glaciers in the European Alps (between 1970 and 1985) was accompanied by shrinkage of small glaciers, which even compensates the gain of area in the class 5 - 10 km^2 by a factor of two, at least for the 165 glaciers selected here. The massive retreat of glaciers since 1985 can be confirmed with the Landsat derived area changes. It is easier to generalize the results of this investigation, because the subdivision of the glaciers into the different area classes is more realistic for glacier retreat than the annually repeated *in situ* length change measurements (especially if applied to the small glaciers).

As a conclusion, more Landsat data should be processed as soon as possible to derive a global glacier inventory and the related changes in recent decades. These data are easy to evaluate for a large number of glaciers, especially in remote areas. They will provide a better statistical basis for further analysis and may clearly exhibit the linkage to the estimated anthropogenic greenhouse forcing. But the importance of glaciers as reservoirs of drinking water, for irrigation, and for energy production purposes also underlines the urgency of such a study. The major obstacle for such an initiative at the moment, is the commercial distribution of the Landsat raw data resulting in enormous costs for a larger number of TM full scenes.

Acknowledgment

I would like to thank Dr. S. Bakan, Max-Planck-Institut für Meteorologie in Hamburg, for support in obtaining the Landsat data used in this study.

References

BAYR, K. J., HALL, D. K. and KOVALICK, W. M., 1994, Observations on glaciers in the eastern Austrian Alps using satellite data, *International Journal of Remote Sensing*, **15**, 1733 - 1742.

DELLA VENTURA, A., RAMPINI, A. and SERANDREI BARBERO, R., 1987, Development of a satellite remote sensing technique for the study of alpine glaciers, *International Journal of Remote Sensing*, **8**, 203 - 215.

DOZIER, J., 1984, Snow reflectance from Landsat 4 Thematic Mapper, *IEEE Transactions on Geoscience and Remote Sensing*, GE - **22**, 323 - 328.

DOZIER, J., 1989, Spectral signature of alpine snow cover from Landsat 5 TM, *Remote Sensing of Environment*, **28**, 9 - 22.

DOZIER, J. and MARKS, D., 1987, Snow mapping and classification from Landsat Thematic Mapper data, *Annals of Glaciology*, **9**, 97 - 103.

GAMPER, M. and SUTER, J., 1978, Der Einfluß von Temperaturänderungen auf die Länge von Gletscherzungen, *Geographica Helvetica*, **33**, 183 -188.

GILLESPIE, A. R., KAHLE, A. B. and WALKER, R. E., 1986, Colour enhancement of highly correlated images: 1. Decorrelation and HSI contrast stretches, *Remote Sensing of Environment*, **20**, 209 - 235.

GRENFELL, T. C., PEROVICH, D. K. and OGREN, J. A., 1981, Spectral albedos of an alpine snow pack, *Cold Regions Science and Technology*, **4**, 121 - 127.

GROSS, G., 1987, Der Flächenverlust der Gletscher in Österreich 1850 - 1920 - 1969, *Zeitschrift für Gletscherkunde und Glazialgeologie*, **23**, 131- 141.

GÜNTHER, R. and WIDLEWSKI, D., 1986, Die Korrelation verschiedener Klimaelemente mit dem Massenhaushalt alpiner und skandinavischer Gletscher, *Zeitschrift für Gletscherkunde und Glazialgeologie*, **22**, 125- 147.

HAEBERLI, W., 1995, Glacier fluctuations and climatic change detection - operational elements of a worldwide monitoring strategie, *WMO - Bulletin*, **44**, 23 -31.

HALL, D. K., ORMSBY, J., BINDSCHADLER, R. A. and SIDDALINGAIAH, H., 1987, Characterization of snow and ice zones on glaciers using Landsat Thematic Mapper data, *Annals of Glaciology*, **9**, 104 - 108.

HALL, D. K., CHANG, A. T. C. and SIDDALINGAIAH, H., 1988, Reflectances of glaciers as calculated using Landsat 5 Thematic Mapper data, *Remote Sensing of Environment*, **25**, 311 - 321.

HALL, D. K., CHANG, A. T. C., FOSTER, J. L., BENSON, C. S. und KOVALICK, W. M., 1989, Com-

parison of in situ and Landsat derived reflectances of Alaskan glaciers, *Remote Sens. Env.*, **28**, S. 493 - 504.

HALL, D. K., BINDSCHADLER, R. A., FOSTER, J. L., CHANG, A. T. C. and SIDDALINGAIAH, H., 1990, Comparison of in situ and satellite derived reflectances of Forbindels Glacier, Greenland, *International Journal of Remote Sensing*, **11**, 493 - 504.

HALL, D. K., WILLIAMS, R. S. and BAYR, K. J., 1992, Glacier recession in Iceland and Austria, *EOS, Transactions of the American Geophysical Union*, **73**, p 129, 135 and 141.

KHOROS, 1991, Software package for digital image processing, V. 1.05), *Khoral Research Inc.*, Albuquerque, New Mexico.

KRIMMEL, R. M. and MEIER, M.F., 1975, Glacier applications of ERTS - 1 images, *Journal of Glaciology*, **15**, 391 - 402.

KUHN, M., 1981, Climate and glaciers, *IAHS*, **131**, 3 - 20.

OERLEMANNS, J., 1994, Quantifying global warming from the retreat of glaciers, *Science*, **264**, 243 - 245.

ØSTREM, G., 1975, ERTS - 1 data in glaciology - an effort to monitor glacier mass balance from satellite imagery, *Journal of Glaciology*, **15**, 403 - 415.

ORHEIM, O. and LUCCHITTA, B.K., 1987, Snow and ice studies by Thematic Mapper and Multispectral Scanner Landsat images, *Annals of Glaciology*, **9**, 109 - 118.

PATERSON, W. S. B., 1981, The physics of glaciers, 2 nd edn (New York: Pergamon Press).

PATZELT, G., 1979-1994, Die Gletscher der Österreichischen Alpen 1978/79 - 1992/93, *Zeitschrift für Gletscherkunde und Glazialgeologie,* **15 - 30**.

PAUL, F., 1995, Fernerkundung von Gletscheränderungen in den Alpen zwischen 1973 und 1992 beobachtet mit Landsat, *Diplomarbeit, Universität Hamburg*, Meteorologisches Institut, **230**.

ROTT, H., 1976, Analyse der Schneeflächen auf Gletschern der Tiroler Zentralalpen aus Landsat Bildern, *Zeitschrift für Gletscherkunde und Glazialgeologie*, **12**, 1 - 28.

ROTT, H. and MARKL, G., 1989, Improved snow and glacier monitoring by the Landsat Thematic Mapper, P*roceedings of a workshop on Landsat Thematic Mapper applications, ESA*, **SP-1102**, pp. 3 - 12.

WARREN, S. G., 1982, Optical properties of snow, *Reviews of Geophysics and Space Physics*, **20**, 67 - 89.

WILLIAMS, R.S., 1987, Satellite remote sensing of Vatnajökull, Iceland, *Annals of Glaciology*, **9**, 119 - 125.

WILLIAMS, R. S., HALL, D. K. and BENSON, C. S., 1991, Analysis of glacier facies using satellite techniques, *Journal of Glaciology*, **37**, 120 - 127.